Nitric Oxide 87 (2019) 31–42

Contents lists available at ScienceDirect

Nitric Oxide

journal homepage: www.elsevier.com/locate/yniox

Increase of cystathionine-γ-lyase (CSE) during late wound repair: Hydrogen sulfide triggers cytokeratin 10 expression in keratinocytes

Itamar Goren*,[1], Yvette Köhler[2], Ahmed Aglan[1], Josef Pfeilschifter, Karl-Friedrich Beck[3], Stefan Frank[3]

Pharmazentrum Frankfurt/ZAFES, Klinikum der Johann Wolfgang Goethe-Universität, Theodor-Stern-Kai 7, D-60590, Frankfurt am Main, Germany

ARTICLE INFO

Keywords:
Wound healing
Hydrogen sulfide
Gene expression
Differentiation
Cytokeratin 10

ABSTRACT

The gaseous mediators nitric oxide (NO), carbon monoxide (CO) and lately also hydrogen sulfide (H_2S) have been described to contribute to the interplay of protein type- and lipid mediators in the regulation of wound healing. In particular, the recently reported role of H_2S in skin repair remains largely unresolved. Therefore we assessed the expressional kinetics of potential H_2S-producing enzymes during undisturbed skin repair: the cystathionine-γ-lyase (CSE), the cystathionine-β-synthase (CBS) and the 3-mercaptopyruvate sulfurtransferase (MPST). All three enzymes were not transcriptionally induced upon wounding and remained silent through the acute inflammatory and proliferative phase of skin repair. By contrast, CSE expression started to increase significantly at the later stages of healing, when cellular proliferation ceases within the granulation tissue and neoepidermis. The importance of H_2S production in late healing phases was supported by a strong induction of otherwise not-induced CBS to complement the loss of CSE function in CSE-deficient mice. Immunohistochemistry revealed hair follicle keratinocytes and basal keratinocytes of the neo-epidermis covering the wound area as sources of CSE expression. Subsequent *in vitro* studies implicated a role of CSE-derived H_2S for keratinocyte differentiation: the H_2S-donor GYY4137 markedly increased the Ca^{2+}-triggered expression of the early keratinocyte differentiation markers cytokeratin 10 (CK10) and involucrin (IVN) in cultured human keratinocytes. Here, GYY4137-derived H_2S strongly enhanced CK10 expression by increasing the binding of RNA polymerase II to the CK10 promoter.

1. Introduction

Nearly two decades ago, the small gaseous molecule nitric oxide (NO) was initially reported to serve an important role during the inflammatory phase of cutaneous wound healing. For the first time in scientific reports on wound healing, there was now the evidence of a gaseous-type mediator that contributed to the complex intercellular communication at the wound site. Even more important, this first seminal study described NO as a pivotal trigger for wound re-epithelialization, as inducible NO synthase (iNOS)-deficient mice showed a severely delayed epithelial wound closure [1]. Consistently, we described the induction of iNOS upon injury and its presence during acute wound inflammation in a mouse model of skin wounding [2]. In particular, it came progressively clear that the small gaseous mediator NO was pivotally linked to keratinocyte biology. NO dose-dependently controlled keratinocyte behavior with respect to proliferation or differentiation [3,4]. Moreover, the functions of NO in keratinocyte biology were found to even expand its initial properties: NO also participated in the release of wound angiogenic [5] as well as neutrophil- and macrophage-specific chemotactic factors [6,7].

A few years later it became evident that NO appeared to be not the single gaseous player in the regulation of tissue movements during skin repair. In 2001, the enzyme heme-oxygenase 1 (HO-1) was first described to be also induced in wound healing [8,9]. Therefore, as HO-1 catalyzes the oxidation of heme to release carbon monoxide (CO), the HO family of enzymes presumably add an additional gaseous mediator

Abbreviations: H_2S, hydrogen sulfide; CSE, cystathionine-γ-lyase; CBS, cystathionine-β-synthase; MPST, 3-mercaptopyruvate sulfurtransferase; CK10, cytokeratin 10; IVN, involucrin; LOR, loricrin; iNOS, inducible nitric oxide synthase; HO, heme oxygenase; ROS, reactive oxygen species

* Corresponding author.
E-mail address: goren@chemie.uni-frankfurt.de (I. Goren).
[1] Present address: Department of Biochemistry, Faculty of Pharmacy, Al-Azhar University, Cairo, Egypt.
[2] *IG and YK contributed equally* to this work.
[3] KB and SF *equally* contributed to this manuscript.

https://doi.org/10.1016/j.niox.2019.03.004
Received 14 November 2018; Received in revised form 30 January 2019; Accepted 6 March 2019
Available online 09 March 2019
1089-8603/

to the wound site [10]. In particular, HO-1 was expressed in a few keratinocytes at the wound margins, but the predominant and major cellular source of HO-1 were infiltrating macrophages during acute repair [8,9]. These studies showed that HO-1 expression itself was not under expressional control of cytokines or growth factors, rather than an additional important species within the group of gaseous mediators: reactive oxygen species (ROS) induced HO-1 expression in keratinocytes [8]. Obviously, also ROS contributed to the increasing group of gaseous mediators in the control of wound healing [11]. However, macrophage-derived HO-1 activity exerted a regulatory role in the release of inflammatory cytokines from the cells [9], a capability that clearly resembles the properties of NO [6,7].

Nevertheless, another gaseous transmitter of intercellular communication was recently introduced to the collection of previously known gaseous mediators. Also hydrogen sulfide (H_2S) was reported to be related to cutaneous wound healing, as H_2S-releasing drugs were capable to improve diabetes-impaired wound tissue in obese mice [12]. Comparable to the identification of NO in the vasculature, first reports on H_2S functions also focused on its role in the vascular system. Here H_2S was described to act as a smooth muscle relaxant acting in synergy with NO itself [13] by opening ATP-dependent K^+-channels in vascular smooth muscle cells [14,15].

It is now well established that H_2S is synthesized by three different enzymes that control the spatial and temporal formation of H_2S in the body. These three enzymes are now known for more than 30 years and involved in cysteine metabolism and transsulfuration pathway [16]. Predominantly expressed in the brain, cystathionine- β-synthase (CBS) is a heme-dependent enzyme. In the presence of cysteine, it drives the formation cystathionine and H_2S [17]. Alternatively, cystathione-γ-lyase (CSE) is capable to use homocysteine and cysteine to release H_2S [18]. Interestingly, the consumption of homocysteine might interfere with cell proliferation, as homocysteine is also the substrate of the methionine synthase, the key enzyme to drive purine biosynthesis. The set of potentially H_2S-producing enzymes is further complemented by mitochondrial enzyme 3-mercaptopyruvate sulfurtransferase (MPST). This enzyme is dependent on the presence of its substrate 3-mercaptopyruvate, which is generated from cysteine and γ-ketoglutarate by activity of the cysteine aminotransferase (CAT).

In view of a potential role of H_2S in the interplay of different gaseous mediators at the wound site, we aimed to gain more basic information concerning the presence of H_2S-releasing enzymes and its possible functions in wound tissue. Here, we report that CSE appeared to be the most relevant H_2S-producing enzyme in wound tissue. Interestingly, CSE expression was delayed beyond the acute inflammatory and proliferative phase of skin repair. The enzyme was significantly induced during late repair, when proliferation of wound cells ceases and final differentiation processes take place. This observation coincides with the expression of CSE in differentiating keratinocytes of the newly formed epidermis and the capability of exogenously applied H_2S to trigger expression of the differentiation marker keratin 10 in keratinocytes.

2. Materials and methods

2.1. Animal experimentation

2.1.1. Animals

Female C57BL/6J (wild-type) and CSE knock out were purchased from GenOway (Hamburg, Germany). At the age of 12 weeks, mice were caged individually using cages with an enriched environment. Prior to wounding, mice were randomly assigned to different experimental groups, monitored for body weight, and wounded as described below.

2.1.2. Wounding of mice

Wounding of mice was performed as described previously [3,5]. Briefly, mice were anesthetized using Ketamin (80 mg/kg) for analgesia and Isofluran (4% vol). Subsequently, six full-thickness wounds (5 mm in diameter, 3–4 mm apart) were made on the backs of the mice by excising the skin and the underlying *panniculus carnosus*. The wounds were allowed to form a scab. Mice were sacrificed by cervical dislocation and subsequent bleeding. An area of 7–8 mm in diameter, which included the granulation tissue and the complete epithelial margins, was excised at the indicated time points for analysis. Back skin from non-wounded mice served as control. Wounds (n = 12) isolated from animals (n = 4) were used for RNA analysis. For protein analysis, wounds (n = 8) from individual mice (n = 4) were used.

2.1.3. Permission

The animal experiments were performed according to the guidelines and approval of the local Ethics Animal Review Board (Regierungspräsidium Darmstadt, D-64278 Darmstadt, Germany). The approval number to this project was V54-19c20/15-FU1055.

2.2. Analysis of gene expression

2.2.1. RNA isolation

RNA isolation was performed as described previously [19]. For the animal experiments, every experimental time point depicts a total of 12 wounds (n = 12) isolated from four individual mice (n = 4) for analysis. For cell culture experiments, every experimental time point depicts the values of three combined plates (n = 3) isolated from three independent cell culture experiments (n = 3).

2.2.2. Reverse-transcription polymerase chain reaction (RT-PCR)

One microgram (1 µg) of total RNA and random hexamer primers were used for MuLV-reverse transcription of cDNA on a T3000-Thermocycler (Biometra, Göttingen, Germany). Primers for the cDNA amplification are described in the following sections.

2.2.3. Quantitative real-time polymerase chain reaction (qRT-PCR)

qRT-PCR was performed to assess the expression of murine CSE, CBS, MPST, CK10, IVN and LOR as well as expression of human CK10 and IVN, respectively. qPCRBIO Mix Lo-ROX was obtained from PCR Biosystems (Nippon Genetics Europe GmbH, Düren, Germany). The predesigned qRT-PCR assays were purchased at Applied Biosystems (Darmstadt, Germany): human IVN (Hs00846307_s1, FAM), human CK10 (Hs01043114_g1, FAM), murine CSE (Mm00461247_m1, FAM), murine CBS (Mm00460654_m1, FAM), murine MPST (Mm00460389_m1, FAM), murine IVN (Mm00515219_s1, FAM), murine LOR (Mm01962650_s1, FAM) and murine CK10 (Mm03009921_m1, FAM). qRT-PCR as performed on an ABI Prism 7500 Fast Sequence Detector (Applied Biosystems) as follows: 95 °C (2 min), 40 cycles: 95 °C (5 s) and 62 °C (30 s). Analyses of qRT-PCR runs were performed by Sequence Detector software. Relative changes in the respective mRNA expression were normalized to human RPLPO (Large Ribosomal Protein) (4310879E, VIC, human cDNA) or to murine GAPDH (4352339E, VIC, mouse cDNA) and quantified by the $2^{-\Delta Ct}$ or $2^{-\Delta\Delta Ct}$ methods.

2.2.4. Preparation of protein lysates

Skin tissue, wound tissue or cultured keratinocytes were homogenized in lysis buffer (1% Triton X-100, 20 mM Tris/HCl pH 8.0, 137 mM NaCl, 10% glycerol, 1 mM DTT, 5 mM EDTA, 10 mM NaF, 2 mM Na_3VaO_4, 1 mM PMSF, 5 ng/ml aprotinin, 5 ng/ml leupeptin, 50 nM okadaic acid). Extracts were cleared by centrifugation. Protein concentrations were determined using the BCA Protein Assay Kit (Fisher Scientific, Schwerte, Germany).

2.2.5. Western blot analysis

Total protein (25–50 µg) was analyzed by SDS gel electrophoresis. After transfer to a nitrocellulose membrane, specific proteins were

detected incubating the respective antibodies (see below) for 16 h at 4 °C. A secondary antibody coupled to horseradish peroxidase (BioRad, Munich, Germany) and the luminol enhancer detection system (Pierce #32106) was used to visualize the proteins.

2.3. Histology

2.3.1. Immunohistochemistry

Wound biopsies were isolated from the back and fixed in formaldehyde buffered solution (4.5% w/v) or frozen in Tissue freezing medium (Leica, Nussloch, Germany) at −80 °C. Wound sections (4 μm) of formaldehyde-fixed and paraffin-embedded tissue were used for immunostaining. Epitopes were retrieved in 10 mM citrate buffer (pH 6.0) by heating at 100°C for 22 min. Sections were incubated over night at 4 °C with antibodies raised against mouse CBS or CSE, and CK10 (see below). Primary antibodies were detected using a biotinylated secondary antibody. The sections were subsequently stained with the avidin-biotin-peroxidase complex system (Santa Cruz, Heidelberg, Germany), the Sigmafast DAB (Sigma, Deisenhofen, Germany) and counterstained with hematoxylin and mounted.

2.4. Cloning

2.4.1. Cloning of the human CK10 promoter for the luciferase reporter assay

Sections of the proximate human CK10 promoter (Homo sapiens chromosome 17, GRCh38.p7; NCBI reference sequence: NC_000017.11) were amplified from HaCaT genomic DNA by PCR using standard protocols. The respective PCR fragments were cloned into pGL3 Basic (Promega, Mannheim, Germany) using the XhoI and HindIII restriction sites. Table 1 provides primer sequences to obtain the CK10 promoter fragments of increasing lengths. Nucleotide numbers indicate primer location relative to the transcriptional start site of the human CK10 gene.

The 2011 nucleotide proximal CK10 promoter region was amplified using 5′-gca tct cga gtt gga aga gtt gca atc tgc-3' (forward) and 5′-cta gca tca ata gtt gcc aca c-3' (reverse) as primer sequences. The amplicon was cloned into pGLK10P1030 (see Table 1) via XhoI-BglII restriction sites to generate pGLK102030. Finally, the SV40 polyadenylation signal of pGLK10P2030 was replaced using the complete 3′-UTR of the human CK10 transcript via XbaI-BamHI restriction sites. The human CK10 3′-UTR was cloned using 5′-gca ttc tag aca aaa cca gag taa tca aga caa tta ttg-3' (forward) and 5′-gca tgg atc cta gtt tgc atc agt aag aaa gtt tat tg-3' (reverse) as primer sequences from human HaCaT keratinocyte cDNA.

2.5. Cell culture

2.5.1. Culturing of human HaCaT keratinocytes

Human HaCaT keratinocytes [20] were cultured in Dulbecco's modified Eagle's medium (DMEM) supplemented with 100 U/ml Pen/Strep (Gibco Life Technologies, ORT, Germany) and heat-inactivated fetal bovine serum (10% v/v) (FBS) (Sigma, Darmstadt, Germany) in a 37 °C humidified environment containing 5% CO_2. Cells were divided once a week at a density of 1.2×10^4 cells per cm^2. For differentiation experiments, keratinocytess were seeded at a density of 5×10^4 cells per cm^2. Cells were exposed to 400 μM GYY4137 as indicated. During the induction experiments using GYY4137, the supernatants were exchanged for fresh GYY4137-containing medium every 24 h. After confluency, cells were differentiated using 2 mM Ca^{2+}.

2.5.2. Transfection of HaCaT keratinocytes for luciferase reporter assays

HaCaT keratinocytes were transfected with CK10 promoter-firefly luciferase reporter vectors along with the renilla luciferase control vector pRL-TK (Promega, Mannheim, Germany) using the Amaxa Nucleofector Cell Line Kit V (Lonza, Basel, Switzerland) according to the manufacturer's protocol. The transfection procedure was done in an Amaxa Nucleofector II device (Amaxa Biosystems, Cologne) using the program A-033. Thereafter, transfected cells were seeded and subsequently cultured to confluence in DMEM supplemented medium. At confluency, cells were differentiated using 2 mM $CaCl_2$ in the absence or the presence of 400 μM GYY4137. To obtain a continuous presence of H2S, GYY3147-supplemnted media were changed every 24 h. Cells were harvested in passive lysis buffer (Promega) and assayed for luciferase activity using the dual luciferase reporter gene system (Promega) in the Glomax 96 microplate luminometer device (Promega). Luciferase activity was normalized to rt renilla control-vector luminescence.

2.5.3. Chromatin immunoprecipitation

Treated HaCaT keratinocytes were fixed in supplemented DMEM medium containing 1% (w/v) formaldehyde for 10 min at room temperature (RT). One volume of glycine buffer (125 mM glycine, 25 mM Tris-HCl pH 7.5 in PBS) was added for 5 min. Cells were subsequently washed with ice-cold PBS and detached from plastic in 1 ml 0.05% (w/v) Trypsin-EDTA at 37 °C for 10 min. Collected cells were washed with ice-cold PBS containing PIC and lysed in 500 μl L1 lysis buffer (10% (v/v) glycerol, 0.1% (v/v) NP40, 2 mM EDTA, 50 mM Tris-HCl pH 8.0 with 2 mM DTT and PIC) for 5 min on ice. Lysed cells pelleted at 900g for 5 min at 4 °C and nuclear pellets were re-suspended in 500 μl L2 lysis buffer (10% (v/v) glycerol, 1% (w/v) SDS, 5 mM EDTA, 50 mM Tris-HCl pH 8.0 with 2 mM DTT and PIC). Samples were placed on ice and chromatin was fragmented by sonication, applying 15 shock pulses (output control grade: 3, 30% duty cycle) at 1 min interval four times using a micro tip sonifier (Branson sonifier 450, G. Heinemann Schwäbisch Gmünd). Nuclear debris was removed by centrifugation at 16,000g for 10 min at 4 °C. Chromatin fragmentation was assessed in 1.5% agarose gel electrophoresis. Samples were divided and diluted (1:10) in Chip DB-dilution buffer (200 mM NaCl, 0.5% (v/v) NP40, 5 mM EDTA, 50 mM Tris-HCl pH 8.0 and PIC). One tenth volume of each sample served as an input loading control. Chromatin-bound α-RNA polymerase II (Pol II) complexes were immunoprecipitated overnight at 4 °C using a mouse monoclonal anti-Pol II antibody and 25 μl protein of G-Sepharose (50% slurry in Chip DB-dilution buffer). A non-specific mouse IgG sample was used as a negative control. The obtained immunoprecipitates were washed on ice using NaCl washing buffer (500 mM NaCl, 0.1% (w/v) SDS, 0.5% (v/v) NP40, 2 mM EDTA and 20 mM Tris-Cl pH 8.0), LiCl washing buffer (500 mM LiCl, 0.1% (w/v) SDS, 0.5% (v/v) NP40, 2 mM EDTA and 20 mM Tris-Cl pH 8.0), and TE buffer (1 mM EDTA and 10 mM Tris-HCl, pH 8.0). Finally, chromatin was eluted in TE buffer containing 2% (w/v) SDS at RT and de-cross-linked with 250 mM NaCl in elution buffer at 65 °C overnight, followed by RNAase A (100 μg/ml) digestion at 65 °C for 30 min. The chromatin solution was adjusted for a final concentration of 10 mM EDTA and 20 mM Tris-HCl, pH 6.5. Proteins were digested with proteinase K (200 μg/ml) at 55 °C for 2 h. Samples were phenol-extracted, ethanol precipitated and recovered in TE. Occupation of α-RNA polymerase II at the CK10 gene TATA region was verified by PCR using the following

Table 1
Oligonucleotides used for cloning of the proximal promoter of human CK10.

plasmid	nucleotides	forward primer	reverse primer
pGLK10P557	−537- +26	gcatctcgagtgtggcaactattgatgctag	gcataagcttggtgatgctgtttagccc
pGLK10P1030	−983- +26	gcatctcgagaacacatgtgcacagtctag	gcataagcttggtgatgctgtttagccc

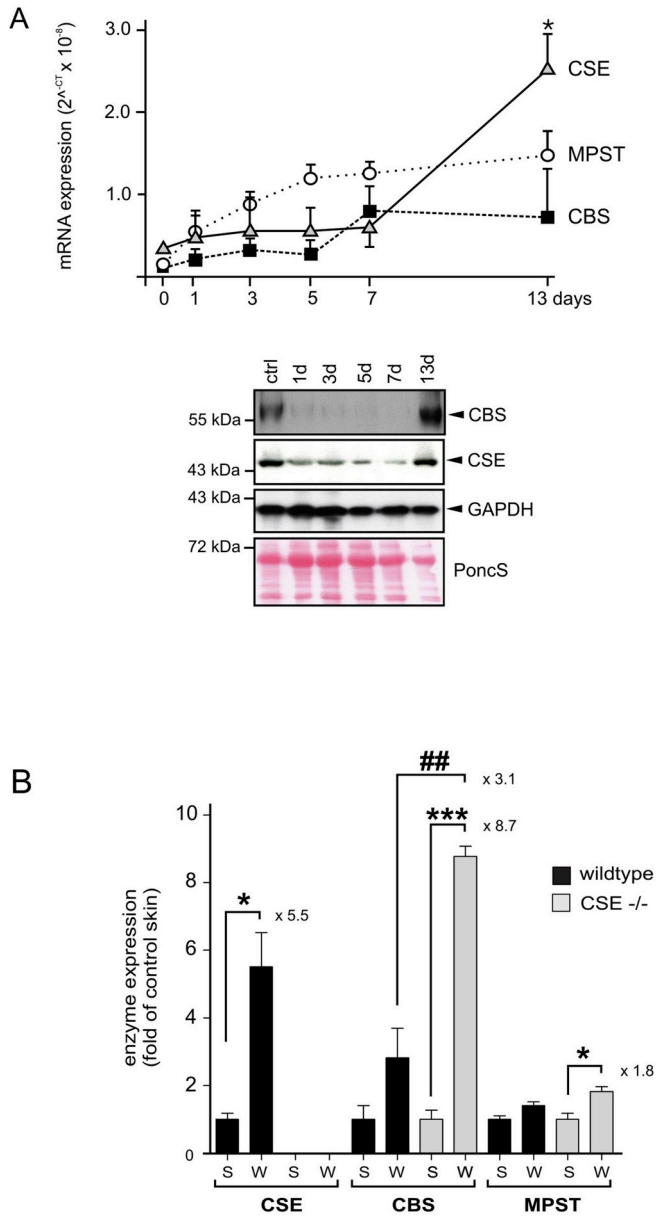

Fig. 1. Expression of H_2S-releasing enzymes during cutaneous wound healing. (A) Quantification of CSE, CBS and MPST mRNA expression during skin repair in C57BL/6J wildtype mice as assessed by qRT-PCR (*upper panel*). Bars indicate the mean ± SD obtained from wounds (n = 3) isolated from four individual animals (n = 4). *$P < 0.05$ (ANOVA) as compared to non-wounded control skin (*day 0*). 50 µg of total protein from control skin (*ctrl*) and wound tissue (*day 1-13*) isolated from C57Bl/6J wildtype mice was analyzed by immunoblot for the presence of CSE and CBS protein expression as indicated (*lower panel*). Every single data point depicts two wounds (n = 2) from four individual animals (n = 4). GAPDH was used to control equal loading. One representative immunoblot is shown. Immunoblot was first analyzed for CSE, then stripped and re-probed for CBS expression. (B) Quantification of CSE, CBS and MPST mRNA expression in non-wounded skin (*Ctrl*) and 13-day wound tissue (*W*) of wildtype (C57Bl/6J) and CSE-deficient mice as indicated. Bars indicate the mean ± SD obtained from wounds (n = 3) isolated from three individual animals (n = 3). **$P < 0.01$; *$P < 0.05$ (Student's unpaired *t*-test) as compared to non-wounded skin (S).

forward (5′-gga ttg gtt att act gaa ga-3′) and reverse (5′-ctt gag ctg tat cga aca ga-3′) primers. Occupation of RNA polymerase II at the GAPDH TATA region was assessed by PCR using the following forward (5′-gga ttg gtt att act gaa ga-3′) and reverse (5′-ctt gag ctg tat cga aca ga-3′) primers. The increase in RNA polymerase II binding at the CK10 TATA region was evaluated on an ABI Prism 7500 Fast Sequence Detector and the qPCRBIO SyGreen Mix Lo-ROX (Nippon Genetics).

2.6. Materials and suppliers

2.6.1. Reagents

Acetic acid (glacial) 100%, Aniline blue, Azocarmine G, Orange G, Phosphotungstic acid, Entellan, Hydrochloric acid (37%), Phenylmethylsulfonyl fluoride (PMSF), dithiothreitol (DTT), aprotinin, NaF, Na_3VaO_4, ethylenediaminetetraacetic acid (EDTA), Sigmafast 3,3′-diaminobenzidine tetrahydrochloride (DAB) (D4168), Aquatex, Protein G-Sepharose and RNAse A were from Sigma (Merck KGaA, Darmstadt, Germany). Leupeptin and ocadaic acid were from BioTrend (Cologne, Germany). Eosin Y solution 0.5% in water and Roti-Histofix, a 4.5% (w/v) formaldehyde buffered solution, were purchased from Roth (Carl Roth GmbH, Karslruhe, Germany). Tissue freezing medium was obtained from Leica (Leica Biosystems, Nussloch, Germany). Mayer's hematoxylin (Part. No. 254766.1611) was obtained from Applichem (Applichem Darmstadt, Germany). GYY4137 was from Cayman (Cayman Chemical, Ann Arbor Michigan, USA). Deoxynucleoside triphosphate, random hexamers, protease inhibitors cocktail (PIC) and Proteinase K were from Roche Diagnostics (Mannheim, Germany). Murine Leukemia Virus (MuLV)-Reverse Transcriptase (RT) was purchased from Applied Biosystems (Thermo Fisher Scientific, Darmstadt, Germany). Proof reading DNA polymerases: Pfu and KAPAHiFi were purchased from Promega (Promega, Mannheim, Germany) and Peqlab, (Peqlab Biotechnology GmbH, Erlangen Germany), respectively. DNA restriction endonucleases were from New England Biolabs (New England Biolabs, Frankfurt, Germany).

2.6.2. Antibodies

Rabbit anti CBS (14787-1-AP) and Rabbit anti CSE (CTH) (12217-1-AP): Proteintech (Acris Antibodies GmbH, Herford, Germany). Mouse monoclonal anti-cytokeratin 1/10 [LH1] (Santa Cruz sc-53251), mouse IgG (Santa Cruz sc-2025) and rabbit IgG (Santa Cruz sc-66931): Santa Cruz, Heidelberg, Germany. Rabbit monoclonal anti-cytokeratin 10 (CK 10) [EP1607IHCY] (ab76318) and mouse monoclonal anti-involucrin (IVN) [SY8] (ab20202): Abcam, Cambridge, United Kingdom. Rabbit anti-involucrin (#924401): Biolegend (Biozol Diagnostica GmbH, Eching, Germany). Rabbit anti-loricrin (LOR) (PRB-145P): Covance Inc. München, Deutschland. Mouse monoclonal anti-GAPDH [GT239]: GeneTex (GTX627408) (Biozo Diagnostica GmbH). Mouse monoclonal anti-RNA polymerase II [CTD4H8] (05-623): Millipore (Merck, Darmstadt, Germany). Horseradish peroxidase (HRP)-conjugated goat anti-mouse IgG (H + L) (170-6516) and HRP-conjugated goat anti-rabbit IgG (H + L) (170-6515): Bio-Rad, Munich, Germany.

2.7. Statistical analysis

Data are shown as means ± SD. Data analysis was performed using the unpaired Student's t-test or analysis of variance (ANOVA) with raw data.

3. Results

CSE is the predominant H_2S-releasing enzyme in skin repair. Although a comprehensive study on H_2S functions to improve diabetes-impaired wound healing is available [12], this study did not provide any information on spatial and temporal expression patterns of the three known H_2S-releasing enzymes. To this end, our analysis on H_2S-releasing enzymes in skin repair was based on the initial determination of CSE, CBS and MPST expression patterns during the course of acute healing upon skin injury, as this information was not available from the literature. As shown in Fig. 1A (upper panel), it became evident that CSE, CBS and MPST were not acutely induced upon skin injury. Although mRNA levels appeared to slightly increase over time, there was

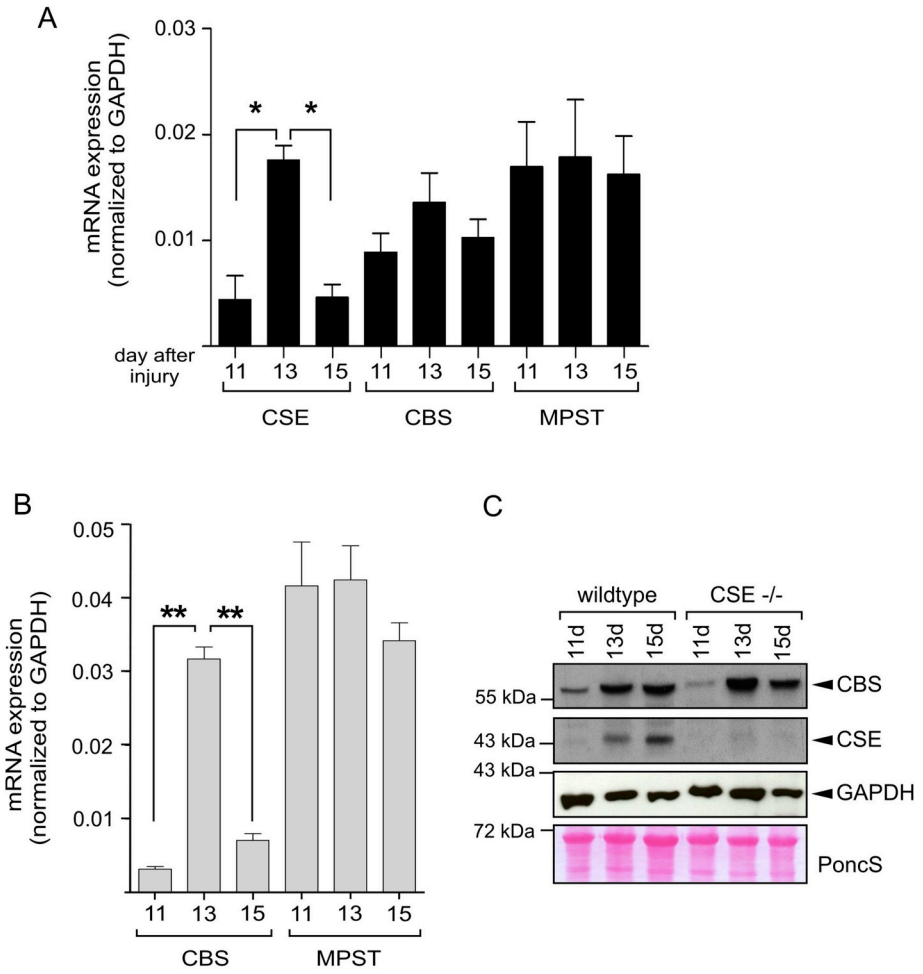

Fig. 2. Expression of CSE, CBS and MPST during late skin repair. Quantification of CSE, CBS and MPST mRNA expression during late skin repair in C57BL/6J wildtype mice (A) and CSE-deficient mice (B) as assessed by qRT-PCR. CSE, CBS and MPST mRNA levels were normalized to GAPDH mRNA. Bars indicate the mean ± SD obtained from wounds (n = 3) isolated from four individual animals (n = 4). $^{**}P < 0.01$ (Student's unpaired *t*-test) as compared to 13-day wounds (*d13*). (C) 50 µg of total protein from wound tissue (*day 11, 13, 15*) isolated from wildtype (C57Bl/6J) or CSE-deficient mice as indicated was analyzed by immunoblot for the presence of CSE and CBS protein expression. Every single data point depicts 2 wounds (n = 2) from three individual animals (n = 3). GAPDH and a Ponceau S (PoncS) staining are shown as a loading controls. One representative immunoblot is shown.

no significant change in CSE, CBS and MPST mRNA levels within the first 7 days of healing. Obviously, the acute inflammatory phase of repair, which is characterized by a marked expressional activation of a wide and diverse number of genes [21,22], did not require the presence of the H_2S-releasing enzymes. However, it is important to note here that expression of particularly one of those enzymes, the CSE, started to increase during late repair. As shown in Fig. 1A, CSE mRNA expression levels started to increase from day 7 and reached a maximum at day 13 of repair (Fig. 1A, upper panel). Thus, CSE appeared to be the unique H_2S-releasing enzyme which is significantly induced during wound healing. By contrast, we observed an only moderate induction of CBS at the mRNA level, reaching its maximum at day 13 post-wounding. That increase in CBS mRNA appeared to be not significant mathematically. Nevertheless, it is tempting to argue here that the observed moderate but 'non-significant' increase in CBS mRNA in late wound tissue does not necessarily exclude a biological consequence, as the observed moderate CBS mRNA levels were actually translated into clearly detectable amounts of CBS protein in late wounds of wildtype (Fig. 1A, lower panels; Fig. 2C) and in CSE −/− mice (Fig. 2C). Highest levels of CSE mRNA were found during the non-proliferative phase following at the end of the acute inflammatory phase of skin repair. Again, immunoblots clearly showed that CSE as well as CBS appeared to play no significant role during wound inflammation (day 1 to day 7), as CSE protein was markedly reduced and CBS protein was missing during that particular phase of repair. However, both enzymes prominently turned up again during late wound healing (Fig. 1A, lower panel). Unfortunately, we could not assess MPST expression, as no functional antibody was currently available.

As a next step, we wounded CSE-deficient mice to learn more about potential functions of the enzyme in wound repair. However, analysis of wound tissue isolated from CSE-deficient mice did not reveal alterations in assessed parameters such as inflammation, granulation tissue formation and the formation of the hyperproliferative wound margin epithelia (data not shown). This observation most likely reflected the absence of CSE induction during the earlier phases of repair. However, expressional analysis of the additional H_2S-releasing enzymes CBS and MPST in wound tissue of CSE-deficient mice indeed strongly suggested a regulatory role of H_2S in late wound tissue. As shown in Fig. 1B, CSE-deficient mice actually aimed to compensate the loss of CSE activity in wound tissue, as late wound tissue showed a marked increase in CBS expression at day 13 post-wounding in those animals. This is even more important, as CBS was not significantly induced at all in undisturbed wound healing (Fig. 1A). In addition, the mitochondrial MPST enzyme did not contribute to the observed compensatory effect of CBS expression (Fig. 1B).

Increased H_2S release appeared to be focused within a small expressional window of CSE expression at day 13 of healing. Analysis of undisturbed wound healing in wildtype mice has revealed a significant increase of CSE expression that was restricted to the late day 13 time point of repair. However, this notion was a result of our basic experimental design. In our mouse model of excisional skin repair [23] (see also Material and Methods), the initial wound size allows a complete granulation and wound re-epithelialization within 13 days of healing. Thus, the day 13 post-wounding time point reflects the latest time point within our standard experimental analyses of wound tissue. Nevertheless, here we were concerned that the significantly elevated levels of CSE at day 13 of healing might not represent the maximum CSE levels, as it was tempting to argue for still increasing CSE

expression beyond day 13 of repair. To this end, wounded an additional series of mice and included a later time point of repair. As shown in Fig. 2A, it became evident that indeed CSE expression levels were highest at day 13 of repair, as we observed a significant decrease of CSE mRNA at day 15 post-wounding. In addition, our data on day 15 of repair confirmed our previous finding that CBS as well as MPST expression was not significantly induced at day 13 of healing and even beyond (Fig. 2A).

As a next step, we repeated that series of experiments using CSE-deficient mice. First, and not unexpected, we could not find any CSE-specific mRNA expression (data not shown) in CSE knock out mice. But it is important to not here that our experiment using CSE-deficient mice again strongly suggested an important role for H_2S in late wound healing. As CSE was absent in wound tissue, CSE-deficient mice showed a marked compensatory induction of the second H_2S-releasing enzyme CSE (Fig. 2B), which was not induced in the presence of an increased CSE expression under late normal wound healing conditions in wildtype mice (Fig. 1). Comparable to CSE expression, the compensatory increase of CBS was also restricted to the day 13 time point of healing (Fig. 2B), suggesting a particular role of the enzymes at that narrow time window of repair. Analyses of CSE and CBS protein expression at late time points confirmed the observed increase in CBS protein in CSE-deficient mice at day 13 of repair (Fig. 2C). The immunoblots indicated an increase in CBS protein in CSE−/− mice when compared to wildtype mice (Fig. 2C), since the CBS signal appeared slightly stronger in CBS-deficient mice. This difference was not as pronounced as the changes at the mRNA level, but still visible. We had to rely on western technique here, as methods for an exact quantification of CBS protein (such as ELISA) are currently not available.

CSE was expressed at hair follicles and within the wound neoepithelium in late wound tissue. Next we determined the localization of CSE protein in late wound tissue (Fig. 3). Wildtype mice showed strong immunopositive signals for CSE protein within matrix keratinocytes of hair follicles (Fig. 3A, left panels and Fig. 3B, upper panel) located in normal non-wounded skin and in hair follicles at the margins of late wound tissue (day 13). An overview of non-wounded skin and 13-day late wound tissue of wildtype and CSE-deficient mice is shown in Supplemental Figs. S1 and S2. Here, the prominent Azan-stained collagen fibers indicate the localization of late granulation tissue. Thus, the marked presence of CSE in hair follicles might account might account for the constitutive expression of CSE protein in non-wounded skin (Fig. 1A). To avoid a misinterpretation of falsely immunopositive signals due to unspecific binding of the anti-CSE antibody in mouse tissue, we also used wound tissue samples from CSE-deficient mice to control the specificity of the CSE staining. CSE-deficient mice lacked a CSE protein expression (Fig. 2C) and should be a useful control to verify the CSE staining in wildtype wound tissue. The non-specific IgG-control experiment did not give any immune-positive signals (Supplemental Fig. S3). As shown in Fig. 3A (right panels), the particularly strong immune-positive signal matrix keratinocytes of the hair follicles was completely absent in CSE knock out mice. Here it is noteworthy that both wildtype and CSE-deficient tissue were developed for the same amount of time (Fig. 3). Staining was prolonged to unequivocally exclude false CSE-positive signals from CSE-deficient skin tissue, which however led to stronger CSE-specific signals in wildtype hair follicles. More important, the use of CSE-deficient mice was even more helpful to identify the rather weak CSE-specific immune-signals in late wound tissue (day 13). Both wildtype and CSE-deficient mice showed a weak staining of the upper keratinocyte layers of within the newly formed neoepithelium, which completely now covered the former wound area (Fig. 3B). Thus, the use of CSE-deficient mice helped to identify those stainings in upper the upper keratinocyte layers as non-specific immune-signals (Fig. 3B, upper panel), as the signals also appeared in the absence of CSE expression (Fig. 2C). Nevertheless, the comparison of stainings within late wildtype and CSE-deficient wound tissue again strongly suggested keratinocytes as the cellular source of CSE expression in 13-day wound tissue. Within the basal layer of the neoepithelium in late wildtype wound tissue, we observed particular keratinocytes which were markedly immune-positive for CSE protein (Fig. 3B, upper panel). Here it is tempting to argue in favor of a reliable CSE staining, as those keratinocyte-specific CSE signals were completely absent in late wound tissue of CSE knock our mice (Fig. 3B, lower panel).

CSE expression in neo-epithelial keratinocytes was temporally paralleled by cytokeratin 10 (CK10) expression. As basal keratinocytes of the wound neoepithelium in late wounds expressed CSE

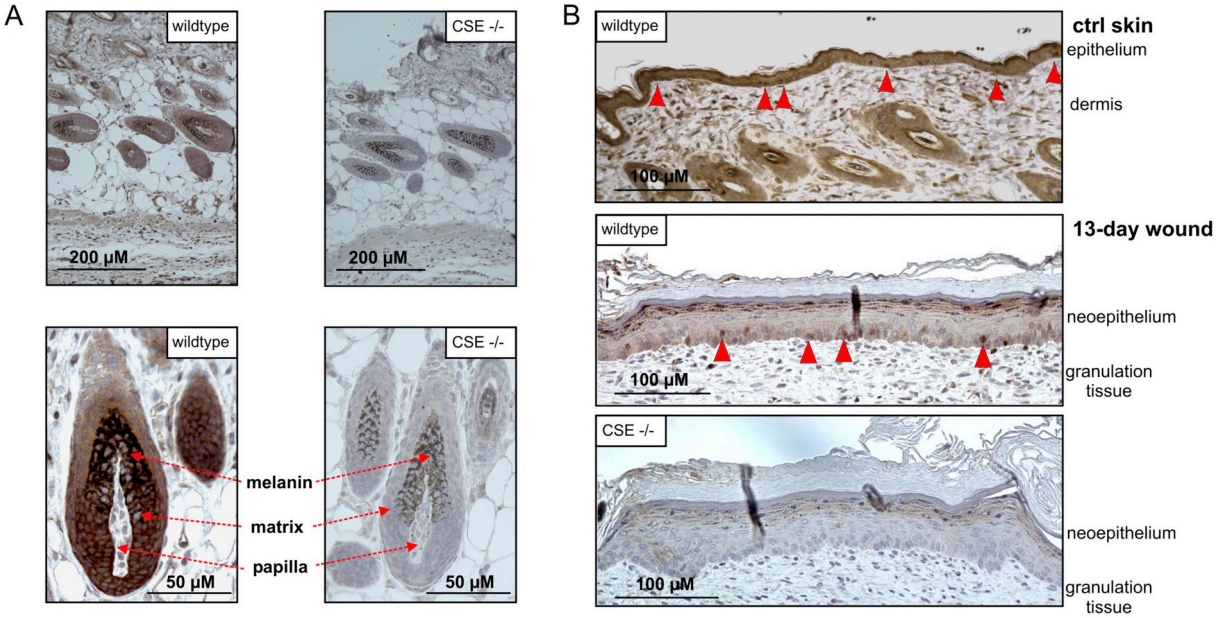

Fig. 3. Localization of CSE protein expression in wound tissue. (A), paraffin sections from directly adjacent wound margin tissue from 13-day wounds isolated from C57Bl/6J *wildtype* mice (n = 3) or CSE-deficient mice (CSE−/−) (n = 3) and (B), non-wounded normal skin of wildtype mice (n = 3) (*upper panel*) and 13-day wound tissue of wildtype (*middle panel*) or CSE-deficient mice (*lower panel*) were incubated with an antibody directed against CSE protein. Immunopositive signals were indicated by red arrows. Scale bars are given in the photographs.

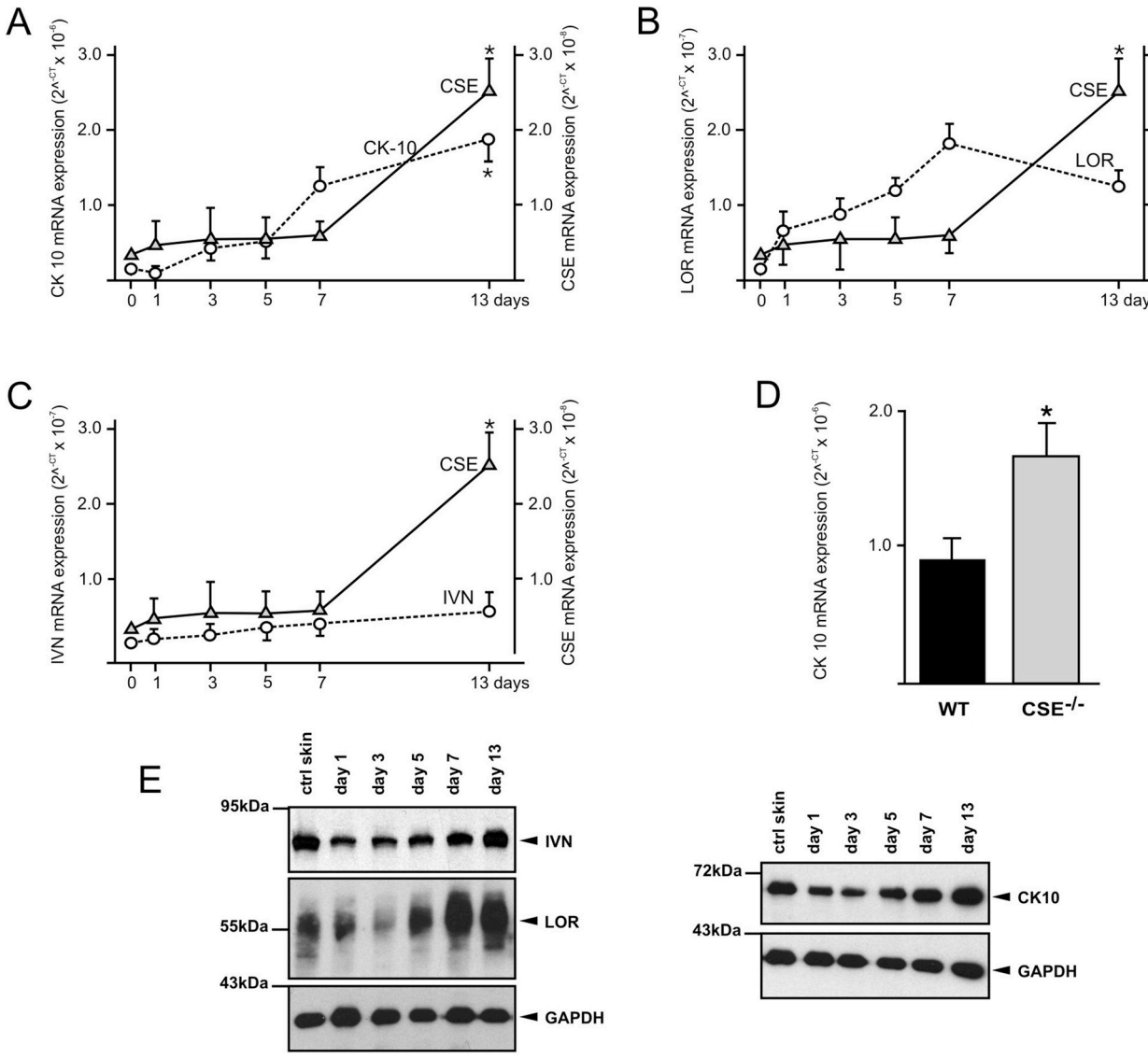

(caption on next page)

Fig. 4. Co-expression of CSE and the differentiation markers CK10, loricin and IVN during wound healing. Quantification of cytokeratin 10 (*CK10*) (A), loricrin (*LOR*) (B), or involucrin (*IVN*) (C) mRNA expression during skin repair in C57BL/6J wildtype mice as assessed by qRT-PCR. Bars indicate the mean ± SD obtained from wounds (n = 3) isolated from four individual animals (n = 4). *$P < 0.05$ (ANOVA) as compared to non-wounded control skin (*day 0*). (D) Quantification of cytokeratin 10 (CK10) mRNA expression in 13-day wounds of C57BL/6J wildtype mice (*WT*) or CSE-deficient mice ($CSE^{-/-}$) as assessed by qRT-PCR. Bars indicate the mean ± SD obtained from wounds (n = 3) isolated from five individual animals (n = 5). *$P < 0.05$ (Student's unpaired *t*-test) as compared to C57BL/6J wildtype mice (*WT*). (E) Total protein (50 µg) from control skin (*ctrl skin*) and wound tissue (*day 1-13*) isolated from C57Bl/6J wildtype mice was analyzed by immunoblot for the presence of involucrin (IVN), loricrin (*LOR*) and cytokeratin 10 (*CK10*) protein expression as indicated. Every single data point depicts 2 wounds (n = 2) from four individual animals (n = 4). GAPDH was used to control equal loading. One representative immunoblot is shown. (F) Paraffin sections from day 13 wound tissue isolated from C57Bl/6J *wildtype* mice or CSE-deficient mice ($CSE^{-/-}$) were incubated with an antibody directed against CK10 protein. Scale bars are given in the photographs. The red line highlights the epidermal margin. CK10 immunopositive signals within the basal keratinocyte layer are indicated by *red arrows*.

(Fig. 3B), we hypothesized a potential role of CSE-released H_2S for keratinocyte differentiation. At day 13 of healing, when CSE levels (and levels of compensatory induced CBS in CSE knock our mice) were highest (Figs. 1 and 2), wound keratinocytes have passed the highly proliferative phase of epithelial hyperproliferation at the wound margins but started to restructure the neo-epithelium by differentiation processes [22,24]. This notion is clearly reflected by the expression of CK10 (Fig. 4A), a marker of final keratinocyte differentiation [25]. Compared to loricrin (LOR) (Fig. 4B) and involucrin (IVN) (Fig. 4C) expression, representing two additional markers of keratinocyte differentiation, particularly CK10 expression appeared to parallel the increase in CSE expression during late wound repair (Fig. 4A). Here it is important to note that the observed induction of the H_2S-releasing enzyme CBS in wound tissue of CSE-deficient mice (Fig. 1B) indeed compensated for the absence of CSE activity, as CK10 mRNA expression levels were not only stabilized but significantly increased in the presence of induced CBS in CSE-knock out mice (Fig. 1D).

In line, IVN, LOR (Fig. 4E, left panel) and CK10 (Fig. 4E, right panel) protein expression started to re-increase from reduced levels, when keratinocytes become important to achieve wound closure by re-epithelialization processes [22,24]. Immunohistochemical stainings of 13-day wound tissue confirmed a potential functional connection of CSE expression in particular neo-epithelial keratinocytes (Fig. 3B, upper panel) and CK10 expression. As shown in Fig. 4F (upper panels), we could find a prominent immunopositive signal for CK10 in the suprabasal keratinocytes of the wound neo-epithelium in wildtype mice. It is important to note that CK10 staining was specific, as the anti-CK10 antibody did not stain the CK10-free cell layer of basal keratinocytes [25]. Here it was pivotal to unequivocally exclude a false immunopositive signal from the anti-CK10 antibody in skin tissue. Despite a prolonged staining for CK10 in wildtype wound tissue (Fig. 4F, upper panel), the antibody did not provide any immunopositive signal in the basal layer of the neo-epithelium. This finding clearly reflects the well-established absence of CK10 expression in basal keratinocytes [25]. This was even more important, as the same anti-CK10 antibody indeed clearly detected signals within the basal layer of CSE-deficient mice, signals from which we now know (due to the absence of signals after prolonged staining of the wildtype wound) that they must be specific and show an unusual expression of CK10 in the basal keratinocyte layer (Fig. 4F, lower panel). Notably, CK10 staining of wound tissue from CSE-deficient mice further supported our data on a compensatory effect of CBS in CSE knock out mice. As shown in Fig. 4F (lower panels), the staining of CK10 did not only stay prominent in 13-day wound tissue of CSE-deficient mice but also clearly extended into the basal keratinocyte cell layer, which should not express CK10 under normal conditions [25].

Hydrogen sulfide (H_2S) amplified Ca^{2+}-induced expression of the keratinocyte differentiation markers cytokeratin 10 (CK10) and involucrin (IVN). As we observed a temporal correlation between the presence of the H_2S-releasing enzyme CSE and CK10 (Fig. 4), we aimed to investigate a potential functional role of H_2S in the regulatory control of CK10 expression. Therefore, we cultured differentiating human HaCaT keratinocytes in the presence or absence of the H_2S-releasing molecule GYY4137 [26]. As shown in Fig. 5A and B, the established Ca^{2+}-stimulus used to drive HaCaT keratinocyte differentiation [20] indeed induced the expression of keratinocyte differentiation markers CK10 and IVN. Notably, the addition of GYY4137 as H_2S-releasing agent was capable to markedly increase the observed Ca2+-induced expression of CK10 (Fig. 5A) as well as IVN (Fig. 5B) in the cells. Nevertheless, the kinetics of H2S-increased CK10 and IVN mRNA levels appeared to be comparably different. Whereas a transient increase in CK10 mRNA, which raised early in differentiation and started to cease from day 2 on, was transformed into a strong and persistent expression by GYY3147 exposure (Fig. 5A), GYY4137 was also capable to significantly advance the expression of IVN mRNA, which showed a long-lasting expression *per se* upon keratinocyte differentiation (Fig. 5B). The GYY3147-mediated increase of Ca^{2+}-induced mRNA expression of both differentiation markers could also be observed at the protein level for CK10 (Fig. 5C) and IVN (Fig. 5D).

A 2000 base pair (bp) promoter fragment proximate to the CK10 transcription start site did not contain gene regulatory elements used by GYY3147. As we had observed a marked increase and also prolongation of Ca^{2+}-induced CK10 expression in keratinocytes (Fig. 5A and C), we were subsequently interested to work out molecular aspects of H_2S actions in the control of CK10 expression. To this end, we cloned three CK10 promoter fragments differing in size, added the luciferase reporter gene, the SV40 polyadenylation signal or the original CK10 3′ untranslated region (UTR) as shown in Fig. 6A (upper panel). However, transcriptional activity of all promoter constructs, independent from length, could not be altered by addition by GYY3147 as shown luciferase reporter activity in an experiment of transient transfection of keratinocytes (Fig. 6, lower panel). This finding strongly indicated that the promoter sequence immediate to the CK10 transcriptional start site did not respond to the presence of H_2S and thus was not sufficient to explain the observed increase in CK10 levels upon GYY3147 exposure (Fig. 5A and C). Here it is important to note that the original CK10 3′ UTR led to a loss of luciferase activity, indicating a destabilizing regulatory element within the CK10 3′UTR. However, also the role of the CK10 3′UTR was not altered by GYY3147 (Fig. 6B).

H_2S enhances binding of RNA polymerase II to the TATA box motif of the CK10 promoter. As 2 kilo bp of the proximate CK10 promoter were not sufficient to explain the distinct H_2S-induced increase in CK10 expression (Fig. 5A and C), we finally analyzed whole promoter activity by chromosome-immunoprecipitation (ChIP) (Fig. 7). To this end, we first designed the respective primer sites to allow later detection of antibody-precipitated TATA promoter sections of the CK10 (Fig. 7A, upper panel) and GAPDH (Fig. 7A, lower panel) genes. As shown in Fig. 7A, both promoter sections contained the respective TATA box of the genes to allow the analysis of transcriptional gene activation through binding of the α subunit of RNA polymerase II (Pol II) to the TATA sequence. Given in Fig. 7B, the comprehensive setting of ChIP now showed that promoter activity of the CK10 gene indeed was responsive to a H_2S signal. PCR analysis of fragments that had been immunoprecipitated by an anti-Pol II antibody clearly showed a regulatory role of H_2S in the control of CK10 gene activity. Notably, the addition of GYY3147 appeared to be an essential prerequisite to enhance CK10 promoter activity in the presence or absence of Ca^{2+}-induced differentiation in keratinocytes (Fig. 7C). Thus, our data strongly

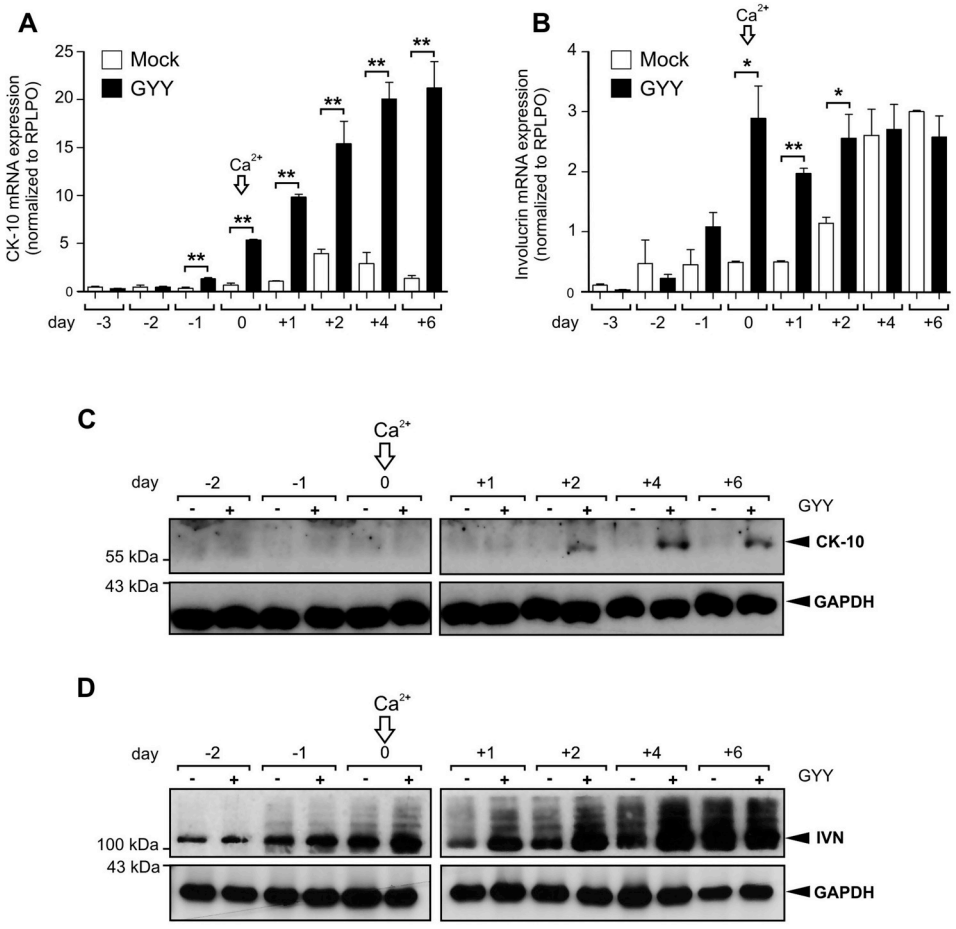

Fig. 5. GYY4137 stimulates CK10 and IVN expression in differentiating cultured human HaCaT keratinocytes. Confluent human keratinocytes (HaCaT) were cultured for three days (*day -3 to -1*). At *day 0*, cells were induced to differentiate by a Ca^{2+}-stimulus (2 mM) as indicated. Quantification of CK10 (A) and IVN (B) mRNA expression in keratinocytes at indicated time points as assessed by qRT-PCR. Bars indicate the mean ± SD obtained from cell culture dishes (n = 3) isolated from three independent experiments (n = 3). $^{**}P < 0.01$; $^{*}P < 0.05$ (Student's unpaired *t*-test) as compared to mock-treated cells. CK10 (C) and IVN (D) protein expression in differentiating HaCaT keratinocytes in the absence or presence of GYY4137 (400 μM) as indicated. GAPDH is shown to control equal loading.

suggested a direct transcriptional enhancement of CK10 expression by stabilizing RNA Pol II binding to the CK10 promoter as an explanation for the observed increase in CK10 expression upon H_2S exposure in keratinocytes.

4. Discussion

Particularly, two most recent reports on biologic functions of H_2S suggested a potential contribution of this gaseous mediator in the process of wound healing. In doing so, both reports complemented the group of tissue-active gaseous mediators that were yet well described to contribute to tissue movements in tissue repair. Two decades ago, the first gaseous mediator in wound repair was identified as NO [1,2], showing a pivotal role in the control of wound keratinocyte proliferation [3] and gene expression [5–7].

The abovementioned recent reports now add H_2S as a regulatory molecule in wound healing. The first study showed an H_2S-mediated improvement of impaired wound healing in the severely diabetic and obese *diabetes/diabetes* (*db/db*) mouse model [12], which served for decades as a reasonable animal model to reproduce diabetes-associated wound healing disorders [27]. Here, H_2S was shown to restore impaired functions of endothelial progenitor cells (EPC) in diabetes-disturbed wound tissue. Stimulation of wound tissue by exogenous application of H_2S-releasing drugs improved overall wound closure rates in the diseased mice. This effect of H_2S was attributed to the preservation of EPC function, leading to an increased expression of angiopoietin-1 and thus a subsequently improved wound skin capillary density [12]. The second recently published study described an effect of H_2S on keratinocyte proliferation and differentiation [28], a cell type pivotal for the control of wound inflammatory [6,7], angiogenic [5,27] and epithelialization [1,3] processes. Interestingly, this study shows that increasing doses of exogenously applied H_2S triggered keratinocyte differentiation, an effect that could be inhibited by siRNA-mediated silencing of autophagy related 5 (ATG5), a key regulatory molecule within the process of autophagy [28].

Here it is now tempting to argue for a role of H_2S that resembles the known actions of NO for keratinocyte biology, as also NO is known to regulate keratinocyte proliferation and differentiation in a dose-dependent manner [4]. In line with the observation that increasing doses of NO triggered keratinocyte differentiation [4], increasing amounts of exogenously applied H_2S also mediated differentiation of cultured keratinocytes [28]. However, the potential effects of CSE and CBS in late stages of wound repair might not fully rely on H_2S release into the regenerating tissue. Both enyzmes are capable to use L-homocysteine as a substrate [18]. To this end, one might hypothesize that CSE and CBS activity also might reduce L-homocysteine levels at the wound site, which is the starting product for the synthesis of 5-S-adenosyl-methionine essential for purine biosynthesis. This suggestion is in accordance to elevated CSE and CBS levels in late repair, when differentiation of new tissue occurs and proliferation of resident wound cells has to cease.

Interestingly, the findings on H_2S-induced keratinocyte differentiation clearly reflect our own data on the temporal expression kinetics of H_2S-releasing enzymes upon skin injury. First, we observed a significant temporal accordance between proliferation-differentiation processes of wound keratinocytes and the levels of CSE expression at the wound site. However, although the observed temporal accordance reflected only a correlation, the restricted increase of CSE during keratinocyte differentiation in late wound epidermis nevertheless argues in favor of a functional link between H_2S and keratinocyte differentiation. This notion is even more supported by the observation that the loss of late CSE activity in CSE-deficient mice was paralleled by a significant increase in

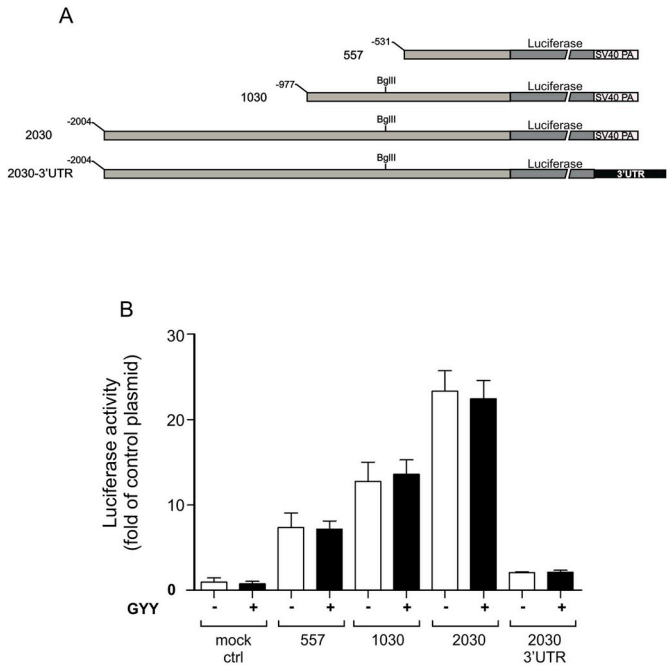

Fig. 6. Activity of the proximate 2030 bp promoter of the CK10 gene is not altered by GYY3147. (A) Constructs used in transfection experiments in HaCaT keratinocytes to analyze for firefly luciferase reporter activity. Constructs 557, 1030 and 2030 carried the SV40 polyadenylation sequence (*SV40 PA*), construct 2030-3′UTR used the 3′UTR isolated from the CK10 gene. (B) HaCaT keratinocytes were transiently transfected with the empty pGL3 plasmid (*mock ctrl*) or the 557, 1030, 2030 and 2030-3′UTR in the absence or presence of GYY4137 (400 µM) as indicated. Luciferase reporter activity was assessed. Bars indicate the mean ± SD obtained from cell culture dishes (n = 3) isolated from three independent experiments (n = 3). Student's unpaired *t*-test as compared to mock-treated cells showed no significance for all analyzed constructs.

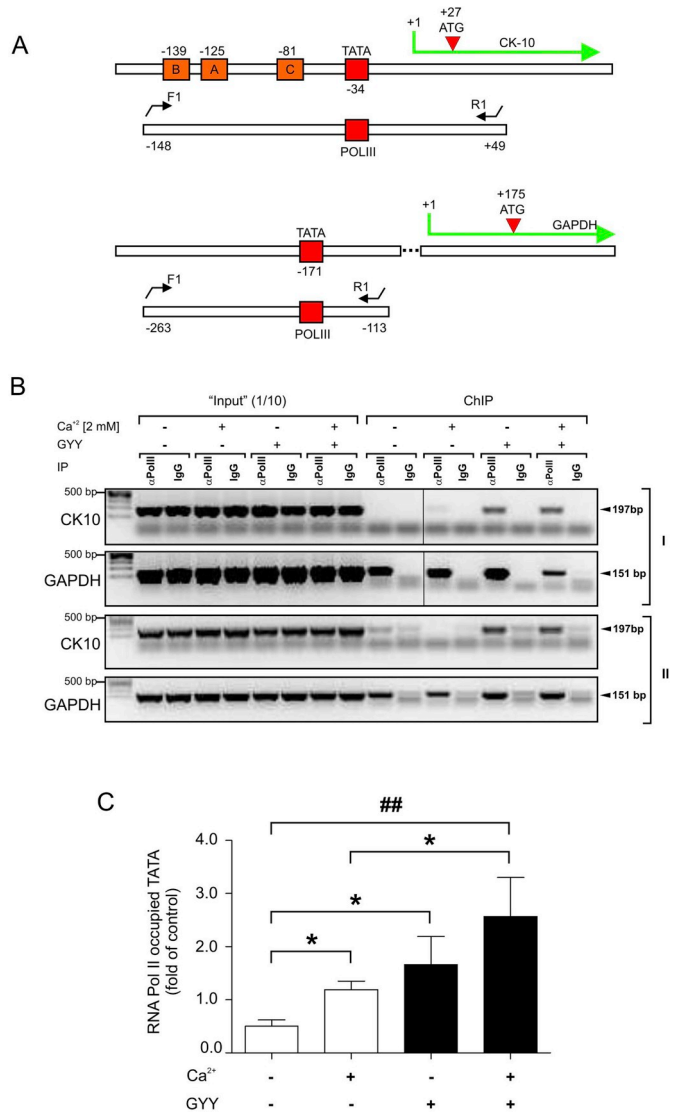

Fig. 7. ChIP analysis of CK10 promoter activity in HaCaT keratinocytes upon GYY4137 stimulation. (A) Localization of promoter-analyzing forward (*F1*) and reverse (*R1*) primers defining the TATA binding site for RNA polymerase II (Pol II) used to analyze CK10 and GAPDH transcriptional activity in ChIP analyses. (B) ChIP analysis of CK10 promoter activity in keratinocytes. Chromatin from Ca^{2+}- and GYY4137-treated cells as indicated was immune-precipitated using an anti-Pol II (Pol II) antibody to detect active transcription. Input depicts analysis of the samples before immune-precipitation. Analysis of constitutively active transcription from the GAPDH promoter was used to as a positive control. (C) Quantification of Pol II binding to the CK10 TATA box in HaCaT keratinocytes in the absence or presence of Ca^{2+} (2 mM) or GYY4137 (400 µM) as assessed by qRT-PCR. Bars indicate the mean ± SD obtained from cell culture dishes (n = 3) isolated from three independent experiments (n = 3). $^{\#\#}P < 0.01$; $^{*}P < 0.05$ (Student's unpaired *t*-test) as indicated by the brackets.

CBS expression in late wound tissue, a H_2S-releasing enzyme that otherwise was only moderately induced in undisturbed wound healing. Although MPST mRNA expression also increased in late wound tissue, it is tempting to argue here for a more restricted role of MPST in healing. MPST is expressed in mitochondria [29]. Even more important, the H_2S-releasing enzymatic activity of MPST is dependent on the activity of the cysteine aminotransferase CAT), which provides 3-mercaptopyruvate as the substrate for MPST activity [30]. As there is no information available on CAT expression in wound tissue yet, and as we have not assessed CAT in our study, it is not clear whether MPST actually contributes to H_2S formation in murine wound tissue.

Although a compensatory up-regulation must be carefully interpreted with respect to CBS function, it is most likely here to suggest a compensatory mechanism in the absence of CSE to provide essential amounts of H_2S to late wound tissue, when wound keratinocytes cease proliferation [3,22,24] and start differentiation during reorganization of the wound neo-epidermis. This notion of a potential H_2S function in keratinocyte differentiation was further supported by the observation that the CK10 marker of early keratinocyte differentiation [25] was also expressed in the basal keratinocyte cell layer upon CBS induction in CSE-deficient mice. It is tempting to argue that the compensatory release of H_2S by CBS was able to stimulate overall wound CK10 expression but failed to control the physiologically restricted superbasal expression pattern of CK10.

Here we provided additional evidence for an indeed functional coupling of H_2S and keratinocyte proliferation. Using the same human keratinocyte cell HaCaT [20], our data confirmed the differentiation effects on HaCaT keratinocytes as reported earlier [28]. By contrast to this study [28], we focused our interest on cellular markers of keratinocyte differentiation such as CK10 and IVN [25]. Notably, expression of both intermediate filaments could be induced by exogenously added H_2S using GYY4137, an established H_2S-releasing molecule [26]. As CK10 gene expression in differentiating mouse epidermis essentially required the transcription factor CCAAT/enhancer-binding-protein (C/EBP) [31,32], we hypothesized that occupation of the C/EBP binding sites within in the CK10 promoter might be primary targets of H_2S actions on the C/EBP transcription factor. The CK10 promoter contains three C/EBP binding sites within the first 170 bp upstream from the transcriptional start site [31]. Thus, as all three C/EBP binding

motifs were contained within our smallest promoter-luciferase reporter construct, which was completely insensitive to H_2S stimulation, our data excluded an obvious interaction of H_2S with these central regulators of keratinocyte differentiation. In addition, the known regulation of nuclear-factor (NF)-κB or NF-E2 p45-related factor 2 (Nrf2) by H_2S could not effect CK10 expression, as the CK10 promoter does not contain both NFκB as well as Nrf2 binding sites. However, when we expanded our analysis to the chromosomal level, we could indeed show an enhanced binding RNA Pol II to the CK10 TATA box (this study). RNA Pol II occupation at the CK10 TATA box is therefore the most general approach to assess the overall potency of H_2S to alter CK10 expression. This observation must not be of minor importance, as the H_2S-mediated RNA Pol II occupation at the CK10 TATA box in keratinocytes was responsible to drive a markedly augmented CK10 expression in the cells. However, our observation of an increased H_2S-driven transcriptional activity with respect to the CK10 promoter is in contrast to published data, which showed an obverse H_2S-mediated inhibition of gene expression by alteration of histone methyl- and acetylation in mouse models of endotoxemia and rheumatoid arthritis [33–35]. These H_2S-driven alterations led to an inhibition of chromatin openness and thus a decrease in gene transcription of inflammatory genes. An additional aspect, which has to be taken into consideration, is the fact that, like NO and reactive oxygen species, H_2S-driven signaling mechanisms act directly on redox-sensitive transcription factors such as Nrf2 or NFκB. For Nrf2, it has been shown that sulfhydration of Kelch-like ECH associated protein 1 (Keap1), the natural inhibitor of Nrf2 on cysteine 151 led to the dissociation and nuclear translocation of Nrf2 and subsequent activation of protective gene expression via the antioxidant responsive element (ARE) in mouse embryonic fibroblasts [36]. Similarly, sulfhydration of the NF-κB subunit p65 on cysteine 38 forces the binding to its co-activator ribosomal protein S3 resulting in an enhanced transcription of NF-κB-dependent genes [37]. However, depending on the complex redox environment and the interaction of H_2S with other gasotransmitters or reactive oxygen species also the inhibition of Nrf2 and NF-kB signaling processes have been reported [reviewed in 29,38]. Moreover, the existence of functional Nrf2 or NF-κB binding sites within the regulatory regions of the CK10 gene is so far questionable and, therefore, it is highly speculative to hypothesize a role for Nrf2 or NF-κB on H_2S-driven CK10 regulation.

In summary, our study for the first time suggests a functional role of the gaseous mediator H_2S in re-epithelialization processes during skin repair. In view of NO, which has been known for decades to dose-dependently regulate keratinocyte proliferation and differentiation during these processes [4], our study suggests H_2S as an additional gaseous mediator in the control of wound keratinocytes in mice.

Acknowledgements

The work was supported by the German Research Foundation (SFB 815, project A7 for JP). AA was supported by grants of the Ministry of Higher Education of the Arab Republic of Egypt.

Appendix A. Supplementary data

Supplementary data to this article can be found online at https://doi.org/10.1016/j.niox.2019.03.004.

References

[1] K. Yamasaki, H.D. Edington, C. McClosky, E. Tzeng, A. Lizonova, I. Kovesdi, D.L. Steed, T.R. Billiar, Reversal of impaired wound repair in iNOS-deficient mice by topical adenoviral-mediated iNOS gene transfer, J. Clin. Investig. 101 (1998) 967–971.

[2] S. Frank, M. Madlener, J. Pfeilschifter, S. Werner, Induction of inducible nitric oxide synthase and its corresponding tetrahydrobiopterin-cofactor-synthesizing enzyme GTP-cyclohydrolase I during cutaneous wound repair, J. Investig. Dermatol. 111 (1998) 1058–1064.

[3] B. Stallmeyer, H. Kämpfer, N. Kolb, J. Pfeilschifter, S. Frank, The function of nitric oxide in wound repair: inhibition of inducible nitric oxide-synthase severely impairs wound reepithelialization, J. Investig. Dermatol. 113 (1999) 1090–1098.

[4] V. Krischel, D. Bruch-Gerharz, C. Suschek, K.D. Kröncke, T. Ruzicka, V. Kolb-Bachofen, Biphasic effect of exogenous nitric oxide on proliferation and differentiation in skin derived keratinocytes but not fibroblasts, J. Investig. Dermatol. 111 (1998) 286–291.

[5] S. Frank, B. Stallmeyer, H. Kämpfer, N. Kolb, J. Pfeilschifter, Nitric oxide triggers enhanced induction of vascular endothelial growth factor expression in cultured keratinocytes (HaCaT) and during cutaneous wound repair, FASEB J. 13 (1999) 2002–2014.

[6] C. Wetzler, H. Kämpfer, J. Pfeilschifter, S. Frank, Keratinocyte-derived chemotactic cytokines. Expressional modulation by nitric oxide in vitro and during cutaneous wound repair in vivo, Biochem. Biophys. Res. Commun. 274 (2000) 689–696.

[7] S. Frank, H. Kämpfer, C. Wetzler, B. Stallmeyer, J. Pfeilschifter, Large induction of the chemotactic cytokine RANTES during cutaneous wound repair: a regulatory role for nitric oxide in keratinocyte-derived RANTES expression, Biochem. J. 347 (2000) 265–273.

[8] C. Hanselmann, C. Mauch, S. Werner, Haem oxygenase-1: a novel player in cutaneous wound repair and psoriasis? Biochem. J. 353 (2001) 459–466.

[9] H. Kämpfer, N. Kolb, M. Manderscheid, C. Wetzler, J. Pfeilschifter, S. Frank, Macrophage-derived heme-oxygenase-1: expression, regulation, and possible functions in skin repair, Mol. Med. 7 (2001) 488–498.

[10] M.D. Maines, The heme oxygenase system: a regulator of second messenger gases, Annu. Rev. Pharmacol. Toxicol. 137 (1997) 517–554.

[11] N. Suzuki, R. Mittler, Reactive oxygen species-dependent wound responses in animals and plants, Free Radic. Biol. Med. 53 (2012) 2269–2276.

[12] F. Liu, D.-D. Chen, X. Sun, H.-H. Xie, H. Yuan, W. Jia, A.F. Chen, Hydrogen sulfide improves wound healing via restoration of endothelial progenitor cell functions and activation of angiopoietin-1 in type 2 diabetes, Diabetes 63 (2014) 1763–1778.

[13] R. Hosoki, N. Matsuki, H. Kimura, The possible role of hydrogen sulfide as an endogeneous smooth muscle relaxant in synergy with nitric oxide, Biochem. Biophys. Res. Commun. 237 (1997) 527–531.

[14] W. Zhao, J. Zhang, Y. Lu, r. Wang, The vasorelaxant effect of H_2S as a novel endogeneous gaseous K_{ATP} channel opener, EMBO J. 20 (2001) 6006–6016.

[15] G. Tang, L. Wu, W. Liang, R. Wang, Direct stimulation of K_{ATP} channels by exogeneous and endogeneous hydrogen sulfide in vascular smooth muscle cells, Mol. Pharmacol. 68 (2005) 1757–1764.

[16] M.H. Stipanuk, P.W. Beck, Characterization of the enzymic capacity for cysteine desulphhydration in liver and kidney of the rat, Biochem. J. 206 (1982) 267–277.

[17] X. Chen, K.H. Jhee, W.D. Kruger, Production of the neuromodulator H_2S by cystathionine beta-synthase via the condensation of cysteine and homocysteine, J. Biol. Chem. 279 (2004) 52082–52086.

[18] S. Singh, D. Padovani, R.A. Leslie, T. Chiku, R. Banerjee, Relative contributions of cystathione beta-synthase and gamma-cystathionase to H_2S biogenesis via alternative trans-sulfuration reactions, J. Biol. Chem. 284 (2009) 22457–22466.

[19] P. Chomczynski, N. Sacchi, Single-step method of RNA isolation by acid guanidinium thiocyanate-phenol-chloroform extraction, Anal. Biochem. 162 (1987) 156–159.

[20] P. Boukamp, R.T. Petrussevska, D. Breitkreutz, J. Hornung, A. Markham, N.E. Fusenig, Normal keratinization in a spontaneously immortalized aneuploid human keratinocyte cell line, J. Cell Biol. 106 (1988) 761–771.

[21] S. Werner, S. Grose, Regulation of wound healing by growth factors and cytokines, Physiol. Rev. 83 (2002) 835–870.

[22] A.J. Singer, R.A.F. Clarke, Cutaneous wound healing, N. Engl. J. Med. 341 (1999) 738–746.

[23] S. Frank, H. Kämpfer, Excisonal wound healing. An experimental approach, Methods Mol. Med. 78 (2003) 3–15.

[24] P. Martin, Wound healing – aiming for perfect skin regeneration, Science 276 (1997) 75–81.

[25] F.M. Watt, Terminal differentiation of epidermal keratinocytes, Curr. Opin. Cell Biol. 1 (1989) 1107–1115.

[26] L. Li, M. Whiteman, Y.Y. Guan, K.L. Neo, Y. Cheng, S.W. Lee, Y. Zhao, R. Baskar, C.H. Tan, P.K. Moore, Characterisation of a novel, water soluble hydrogen sulfide releasing molecule (GYY4137): new insights into the biology of hydrogen sulphide, Circulation 117 (2008) 2351–2360.

[27] S. Frank, G. Hübner, G. Breier, M.T. Longaker, D.G. Greenhalgh, S. Werner, Regulation of vascular endothelial growth factor expression in cultured keratinocytes. Implications for normal and impaired wound healing, J. Biol. Chem. 270 (1995) 12607–12613.

[28] X. Xie, H. Dai, B. Zhuang, L. Chai, Y. Yie, Y. Li, Exogenous hydrogen sulfide promotes cell proliferation and differentiation by modulating autophagy in human keratinocytes, Biochem. Biophys. Res. Commun. 472 (2016) 437–443.

[29] S. Longen, K.F. Beck, J. Pfeilschifter, H2S-induced thiol-based redox switches: biochemistry and functional relevance for inflammatory diseases, Pharmacol. Res. 111 (2016) 642–651.

[30] N. Shibuya, S. Koike, M. Tanaka, M. Ishigami-Yuasa, Y. Kimura, Y. Ogasawara, K. Fukui, N. Nagahara, H. Kimura, A novel pathway for the production of hydrogen sulfide from D-cysteine in mammalian cells, Nat. Commun. 4 (2013) 1366–1372.

[31] E.V. Maytin, J.C. Lin, R. Krishnamurthy, N. Batchvarova, D. Ron, P.J. Mitchell, J.F. Habener, Keratin 10 gene expression during differentiation of mouse epidermis requires transcription factors C/EBP and AP-2, Dev. Biol. 216 (1999) 164–168.

[32] E. Sterneck, S. Zhu, A. Ramirez, J.L. Jorcano, R.C. Smart, Conditional ablation of C/EBP beta demonstrates its keratinocyte-specific requirement for cell survival and mouse skin tumorigenesis, Oncogene 25 (2006) 1272–1276.

[33] E.C. Rios, B. Szczesny, F.G. Soriano, G. Olah, C. Szabo, Hydrogen sulfide attenuates

cytokine production through the modulation of chromatin remodeling, Int. J. Mol. Med. 35 (2015) 1741–1746.
[34] W. Wu, M. Qin, W. Jia, Z. Huang, Z. Li, D. Yang, M. Huang, C. Xiao, F. Long, J. Mao, P.K. Moore, X. Liu, Y.Z. Zhu, Cystathione-γ-lyase ameliorates the histon demethylase JMJD3-mediated autoimmune response in rheumatoid arthritis, Cell. Mol. Immunol. (2018 May 29), https://doi.org/10.1038/s41423-018-0037-8 ([Epub ahead of print]).
[35] S. Liu, X. Wang, L. Pan, W. Wu, D. Yang, M. Qin, W. Jia, C. Xiao, F. Long, J. Ge, X. Liu, Y. Zhu, Endogenous hydrogen sulfide regulates histone demethylase JMJD3-mediated inflammatory response in LPS-stimulated macrophages and in a mouse model of LPS-induced septic shock, Biochem. Pharmacol. 149 (2018) 153–162.
[36] G. Yang, K. Zhao, Y. Ju, S. Mani, Q. Cao, S. Puukila, N. Khaper, L. Wu, R. Wang, Hydrogen sulfide protects against cellular senescence via S-sulfhydration of Keap1 and activation of Nrf2, Antioxidants Redox Signal. 18 (2013) 1906–1919.
[37] N. Sen, B.D. Paul, M.M. Gadalla, A.K. Mustafa, T. Sen, R. Xu, S. Kim, S.H. Snyder, Hydrogen sulfide-linked sulfhydration of NF-κB mediates its antiapoptotic actions, Mol. Cell. 45 (2012) 13–24.
[38] A. Giuffrè, J.B. Vicente, Hydrogen sulfide biochemistry and interplay with other gaseous mediators in mammalian physiology, Oxid. Med. Cell. Longev. 2018 (2018).